



PCCP

Enhancement of Oxygen Reduction Reactivity on TiN by Tuning the Work Function via Metal Doping

Journal:	<i>Physical Chemistry Chemical Physics</i>
Manuscript ID	CP-COM-09-2022-004326.R1
Article Type:	Communication
Date Submitted by the Author:	08-Nov-2022
Complete List of Authors:	Chisaka, Mitsuharu; Hirosaki University, Department of Sustainable Energy Abe, Toshiyuki; Hirosaki University, Department of Frontier Materials Chemistry, Graduate School of Science and Technology Xiang, Rong; The University of Tokyo, Mechanical Engineering; Zhejiang University, State Key Laboratory of Fluid Power and Mechatronic Systems, School of Mechanical Engineering Maruyama, Shigeo; The University of Tokyo, Department of Mechanical Engineering Daiguji, Hirofumi; The University of Tokyo, Department of Mechanical Engineering

SCHOLARONE™
Manuscripts

PCCP

COMMUNICATION

Enhancement of Oxygen Reduction Reactivity on TiN by Tuning the Work Function *via* Metal Doping

Mitsuharu Chisaka,^{*a} Toshiyuki Abe,^b Rong Xiang,^{c,d} Shigeo Maruyama^d and Hirofumi Daiguji^d

Received 00th January 20xx,

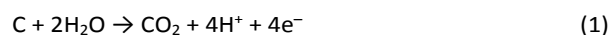
Accepted 00th January 20xx

DOI:10.1039/x0xx00000x

Oxide layers on conductive TiN have recently been investigated to catalyse the oxygen reduction reaction (ORR) in acidic media. The ORR reactivity, *i.e.*, activity and selectivity, has been correlated with the surface nitrogen atoms. A new strategy, optimising the work function *via* the doping of foreign metals, is revealed herein to enhance the reactivity.

Polymer electrolyte fuel cells (PEFCs) have already been commercialised in various transport and residential applications, including in passenger vehicles, buses, trucks, forklifts, and in systems that cogenerate power and heat in houses. New applications are expected in the heavy-duty transportation sectors, in trains, aircraft and ships.¹ However, the standing of PEFCs in all the existing markets remains niche. The use of platinum catalysts in both the anode and cathode of PEFCs is assumed to be the highest cost barrier that hinders the widespread use of PEFCs.² Decreasing platinum usage may thus contribute to the existing market growth in the near future, with the US Department of Energy having set a target limit of 0.1 grams of platinum group metals (PGMs) per kilowatt by 2025.³ The development of PGM-free catalysts can accelerate both the existing market expansion and the launch of markets for new applications, as mentioned above. However, since the late 2000s, only two types of PGM-free catalysts have been developed to catalyse the oxygen reduction reaction (ORR) at PEFC cathodes, where currently four times higher platinum loading is required compared with the anode counterparts that catalyse the faster hydrogen oxidation reaction (HOR).⁴ One is the so-called M/N/C catalysts, in which M = Fe, Co or Mn are coordinated with nitrogen (N) atoms at the edge of defective graphitic carbons (C).^{5–7} After the breakthrough demonstration of Fe/N/C catalyst activity by the Dodelet group,⁵ focus has been

on developing M/N/C catalysts.^{6,7} Recently, the use of PGMs for the metal site such as Ir/N/C and Rh/N/C has been proposed.⁸ The other is oxide catalysts with group IV or V metals,^{9–15} which have the advantage of high chemical stability and do not dissolve in the acidic environment of PEFCs.¹⁰ However, they exhibit poor conductivity that inhibits their activity evaluation, even in screening the catalyst candidates in a half cell in liquid electrolytes.⁹ To remedy this, conductive carbon materials have been used as supports.^{11–13} The best single-cell performance delivered by zirconium oxynitride on multiwalled carbon nanotubes (MWCNTs)¹² attracted the attention of the Dodelet group,⁷ while the stability was insufficient even when the cell was operated at ≤ 1 V. At a potential of ≥ 0.207 V relative to a standard hydrogen electrode, carbon species can be oxidized to form carbon dioxide according to eq. (1):



Our group has focused on oxide layer catalysts formed on metallic TiN, which were originally synthesised on carbon black supports,¹³ with the ORR activity boosted by removing the carbon black due to the active TiN being highly conductive.¹⁴ Both the activity and durability of TiN have recently been enhanced *via* doping with zirconium (Zr) as Zr (1) distorts the TiN lattice to create active sites and (2) inhibits crystallite growth to increase surface area during high-temperature synthesis.¹⁵ The catalyst with the optimised composition, $\text{Ti}_{0.8}\text{Zr}_{0.2}\text{O}_x\text{N}_y$ delivered high durability during 5,000 startup/shutdown cycles to display only 0.04 V decrease in halfwave potential.¹⁵ The durability is the merit of this catalyst when compared with M/N/C catalyst which significantly degraded due to the oxidation of carbon species.¹⁶ However, the initial activity should be enhanced further for the practical use. Doping using metals with different ionic radii is an attractive pathway by which to control the crystal structure of metal oxide/nitride compounds in the field of photocatalysis, coatings and hydrogenolysis.¹⁷ However, dual metal oxide or nitride ORR catalysts for use in acidic electrolytes have rarely been investigated. In this study, four metals were doped into TiN-based catalysts to clarify the role played by the dopants in the ORR reactivity.

^a Department of Sustainable Energy, Hirosaki University, 3 Bunkyo-cho, Hirosaki, Aomori 036-8561, Japan. E-mail: chisaka@hirosaki-u.ac.jp

^b Department of Frontier Materials Chemistry, Graduate School of Science and Technology, Hirosaki University, 3 Bunkyo-cho, Hirosaki, 036-8561 Japan.

^c State Key Laboratory of Fluid Power and Mechatronic Systems, School of Mechanical Engineering, Zhejiang University, Hangzhou 310027, China.

^d Department of Mechanical Engineering, The University of Tokyo, 7-3-1 Hongo, Bunkyo-ku, Tokyo 113-8656, Japan.

† Electronic Supplementary Information (ESI) available: [Experimental details, X-ray photoelectron spectra, electrochemical measurement results, X-ray diffraction patterns, backscattered electron images, energy dispersive X-ray spectroscopy mappings]. See DOI: 10.1039/x0xx00000x

Zr, niobium (Nb), nickel (Ni) and vanadium (V) were selected as TiN dopants, with all of the dual nitrides synthesised *via* combustion,^{13–15} as detailed alongside the characterisation of the materials in S1, ESI†. As the surface of TiN is oxidised by moisture in the air,¹⁸ the catalysts were denoted as $Ti_{1-d}M_dO_xN_y$, with the doping level d of M (Zr, Nb, Ni or V) fixed at 0.2, the optimum value for the reactivity of $Ti_{1-d}Zr_dO_xN_y$.¹⁵ The d values evaluated with energy dispersive X-ray spectroscopy (EDS) were in good agreement with the nominal value, 0.2 (S1, ESI†). Fig. 1 shows X-ray diffraction (XRD) patterns of the catalysts, which exhibit a TiN phase with impurities created by the dopants. $Ti_{0.8}Zr_{0.2}O_xN_y$ contains tetragonal and monoclinic ZrO_2 phases, while $Ti_{0.8}Nb_{0.2}O_xN_y$ and $Ti_{0.8}Ni_{0.2}O_xN_y$ contain rutile TiO_2 and metallic Ni phases, respectively. Only $Ti_{0.8}V_{0.2}O_xN_y$ displays a single TiN phase, which suggests that the amount of V ions dissolved into the TiN lattice is the highest among the four dopants. The ionic radii of Ti^{3+} , Zr^{3+} , Nb^{3+} , Ni^{3+} , and V^{3+} are 0.067, 0.089, 0.072, 0.056–0.060, and 0.064 nm, respectively.¹⁹ As the ionic radii of V^{3+} is the closest to that of Ti^{3+} compared to the other dopants, the V species do not segregate to form oxides, metals or other compounds. Indeed, the TiN (2 0 0) peak of $Ti_{0.8}V_{0.2}O_xN_y$ is higher than that of any of the other catalysts (S2, ESI†), suggesting that the substitution of small V^{3+} for Ti^{3+} in TiN contracts the TiN lattice. As shown in Fig. 1(iii), the dissolution of Ni^{3+} in TiN is low, with the formation of Ni metal, so that the TiN (2 0 0) peak is not shifted to a higher angle compared to that of $Ti_{0.8}V_{0.2}O_xN_y$ (S2, ESI†), despite Ni^{3+} having the smallest ionic radius.

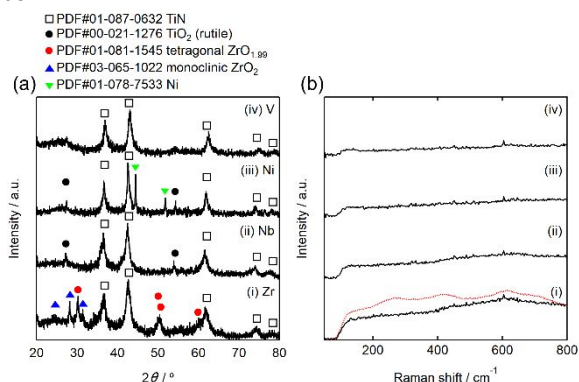


Fig. 1 (a) X-ray diffraction (XRD) patterns and **(b)** ultraviolet (UV) Raman spectra of the four metal-doped titanium oxynitride, $Ti_{0.8}M_{0.2}O_xN_y$ catalysts, where M = (i) Zr,¹⁴ (ii) Nb, (iii) Ni and (iv) V. All catalysts were synthesised *via* pyrolysis at 1173 K for 2 h under N_2 gas. As a reference, a UV Raman spectrum of commercial rutile TiO_2 powder is shown as a dashed line in (b)–i. Compared to the differences in the bulk crystal structures, the crystal structures of the top surfaces of the four catalysts, as shown in Fig. 1(b), were evaluated by ultraviolet (UV) Raman spectroscopy and were found to be similar. Compared with XRD or visible Raman spectroscopy using a 532 nm laser, UV Raman spectroscopy using a 325 nm laser is more sensitive to surfaces as surface oxides strongly absorb UV laser light.²⁰ We have previously shown that TiN on the surface of $Ti_{0.8}Zr_{0.2}O_xN_y$ evaluated by visible Raman spectroscopy with a 532 nm laser is oxidised to a rutile TiO_2 phase by moisture in the air.¹⁵ The UV Raman spectrum shown in Fig. 1 (b)–i is clearly different from that of rutile TiO_2 powder measured under the same conditions, indicated by the dashed line. The broad and small peaks at around 600 cm^{-1} are both typical features of an amorphous TiO_2 phase.²¹ The other metal doped catalysts also exhibit similar UV

Raman spectra, as shown in Fig. 1(b)–ii–iv, indicating that the top surfaces of the four catalysts were oxidised to form amorphous oxides, mostly TiO_2 .

The morphology of the catalysts was investigated using field emission scanning electron microscopy (FE-SEM). Both $Ti_{0.8}Zr_{0.2}O_xN_y$ and $Ti_{0.8}Nb_{0.2}O_xN_y$ exhibit similar uniform fine particles, as shown in Fig. 2(i) and (ii), respectively. Compared to these two catalysts, $Ti_{0.8}Ni_{0.2}O_xN_y$ exhibits a denser morphology as shown in Fig. 2(iii), mostly originating from TiN particle aggregation and smaller Ni metal particles are observed on the TiN surface (S3, ESI†). In Fig. 2(iv), sheets can be observed only for $Ti_{0.8}V_{0.2}O_xN_y$, indicating that dissolved V ions interconnect the particles. Similar results were reported by Yao and Wang²² and Chang *et al.*²³ for V-doped TiO_2 as an electrode for sodium ion batteries and a catalyst for the degradation of azo dyes, respectively.

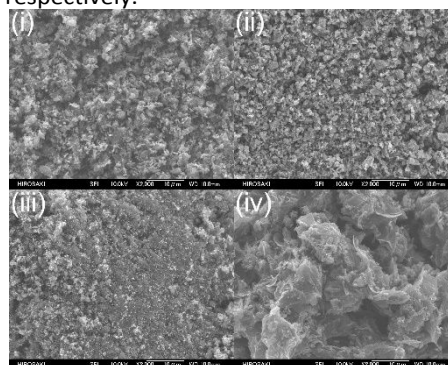
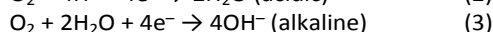


Fig. 2 Field emission scanning electron microscopy (FE-SEM) images of the four $Ti_{0.8}M_{0.2}O_xN_y$ catalysts, where M = (i) Zr, (ii) Nb, (iii) Ni and (iv) V.

XRD, UV Raman spectroscopy and FE-SEM analyses show that an amorphous TiO_2 layer is formed on the top surface of bulk TiN for all four catalysts, with the morphology dependent on the doped metals. As shown in Fig. 3(A), despite their similar surface crystal structures, the four catalysts display different activities in the surface ORR. Above 0.6 V, which is the practical potential range for automotive PEFCs,²⁴ the ORR activity of the $Ti_{0.8}M_{0.2}O_xN_y$ catalysts was found to be strongly dependent on M in the order of $V \ll Ni < Nb < Zr$. It is noted that metallic Ni observed from Fig. 1(a)–iii dissolved into the electrolyte during the electrochemical measurements, and thus, the activity of $Ti_{0.8}Ni_{0.2}O_xN_y$ shown in Fig. 3(A)–iii is not from the metallic Ni (S4, ESI†). Since the ORR activity of M-free TiO_xN_y catalysts is highly dependent on the nitrogen doping level on the outer surface of TiO_2 ,^{13,14} the y values were evaluated using X-ray photoelectron spectroscopy (XPS, S1, ESI†). The kinetic current density, j_k , and the number of electrons transferred per unit oxygen molecule, n , were evaluated at 0.7 and 0.6 V, respectively (S1, ESI†) and they were plotted as a function of y , as shown in Fig. 3(B), to reveal the effect of y on the ORR activity and selectivity of the $Ti_{0.8}M_{0.2}O_xN_y$ catalyst, respectively. Both j_k and n show no clear dependence on y , indicating that the dominant factor in the ORR for $Ti_{0.8}M_{0.2}O_xN_y$ catalysts was different from that for TiO_xN_y catalysts without M. To determine the cause of the intrinsic reactivity of the ORR, the work function, Φ , of the four $Ti_{0.8}M_{0.2}O_xN_y$ catalysts was evaluated by photoemission yield spectroscopy in air (PYSA). PYSA was chosen as it can be used to determine Φ quickly in air without damaging the catalysts during measurements with high repeatability, and the standard deviation is 0.02 eV. j_k was found to be independent of Φ , while

n was dependent on Φ , reaching a maximum at around 5.0 eV, indicating that there is an optimum Φ for the ORR selectivity to the four-electron reaction ($\text{O}_2 + 4\text{H}^+ + 4\text{e}^- \rightarrow 2\text{H}_2\text{O}$). Φ is the difference in potential energy of an electron between the vacuum and Fermi levels, which corresponds to the minimum energy required to extract an electron from a solid surface and can be correlated to the ORR reactivity of non-PGM catalysts. Cheon *et al.*²⁵ were the first to investigate the effect of Φ on the ORR reactivity of non-PGM catalysts, reporting that the ORR activity and selectivity of nitrogen, sulfur, and oxygen tri-doped carbon catalysts in alkaline media increased upon decreasing Φ , as measured by Kelvin probe force microscopy. This occurs due to doped carbons with a small Φ having a low energy barrier to donate electrons from the catalyst surface to adsorbed oxygen, thereby promoting the ORR. Although the ORR activity of the doped carbon catalysts in acidic media was observed below 0.6 V, similar trends have been reported, with both j_k and n in acidic media increasing with decreasing Φ from 5.0 to 4.8 eV.²⁵ Since then, several other groups have drawn similar conclusions. Sharma *et al.* reported graphene layers formed on cobalt nanoparticles and found the source of ORR activity in alkaline media to be a low Φ value of 3.18 eV, calculated using spin-polarized density functional theory (DFT).²⁶ Nandan *et al.* synthesised two different bimetallic FeCo crystals encapsulated in nitrogen-doped carbon. They reported that the face-centred cubic (FCC) phase of FeCo exhibited higher ORR activity and selectivity in alkaline media than the body-centred cubic (BCC) phase due to the Φ measured by ultraviolet photon spectroscopy (UPS) being 0.2 eV smaller, 4.52 eV for the FCC phase and 4.72 eV for the BCC phase.²⁷ Shin *et al.* reported that the ORR activity of sulfur-doped carbon catalysts in alkaline media increased with decreasing Φ from 5.22 to 5.07 eV, as measured by UPS.²⁸ These previous studies focused on carbon-based non-PGM catalysts for alkaline media, with reported higher ORR activity than in acidic media. In acidic and alkaline media, the ORR proceeds *via* different pathways:



and the ORR mechanism is different in these two media. This study is the first to demonstrate an experimentally determined optimum Φ of approximately 5.0 eV for the ORR selectivity of $\text{Ti}_{0.8}\text{M}_{0.2}\text{O}_x\text{N}_y$ catalysts in acidic media. Recently, Zhao *et al.*

found that the optimum $\text{SmMn}_2\text{O}_{5-6}$ catalyst for the ORR in neutral media has a Φ value of around 6.12 eV *via* DFT calculations.²⁹ They reported that if the magnitude of Φ is too small, the catalyst-ORR intermediate interaction becomes stronger and ultimately slows down the ORR process. The ORR mechanism in neutral media was assumed to proceed *via* eq. (3), with the intermediate being HO_2 ,²⁹ the same as that in acidic media (S5, ESI^+). Indeed, HO_2 intermediates and M-doped TiO_2 bind strongly to $\text{Nb} < \text{V} < \text{Ni}$ in that order, from DFT calculations.³⁰ Besides this interaction between the reaction intermediate and the catalyst, it has been noted that the smaller the Φ , the more negative potential at which the ORR proceeds.³¹ This could be one of the reasons for the decrease in the ORR selectivity with a decrease in Φ . The Φ was decreased, i.e., the Fermi level of TiN was upshifted by doping foreign metals with the following order $\text{Nb} > \text{Zr} > \text{V} > \text{Ni}$. Either Zr or Nb was close to the optimum for tuning the Fermi level to donate electrons to O_2 molecules and not to bind strongly with the reaction intermediate at the potential where ORR proceeds. As j_k is a kinetic parameter, it was not possible to determine its value using only the static parameter Φ . In addition to the above factors determining n , the morphology of the catalysts could contribute to determining the trend of j_k . Figure 2 shows that $\text{Ti}_{0.8}\text{Zr}_{0.2}\text{O}_x\text{N}_y$ and $\text{Ti}_{0.8}\text{Nb}_{0.2}\text{O}_x\text{N}_y$ are composed of uniform fine particles, while $\text{Ti}_{0.8}\text{Ni}_{0.2}\text{O}_x\text{N}_y$ and $\text{Ti}_{0.8}\text{V}_{0.2}\text{O}_x\text{N}_y$ are not uniform, each exhibiting a high-density morphology and a sheet shape, respectively. These uniform fine particle morphologies could contribute to the increase in j_k by increasing the surface area of the particles and decreasing the contact resistance compared to the non-uniform particles. The activity trend does not change even after compensating the effect of surface area of four catalysts and after optimising the d for $\text{Ti}_{1-d}\text{Nb}_d\text{O}_x\text{N}_y$ (S6, ESI^+). Among the four metal dopants used in this study, Zr was the best at maximising reactivity from two aspects: (1) tuning Φ to increase the ORR selectivity for four-electron reactions and (2) producing uniform fine particles to increase the ORR activity. Besides, a small amount of tetragonal ZrO_2 phase shown in Fig. 1(a)-i could assist the ORR activity.¹² Our previous study showed that some of the Zr ions dissolve in the TiN lattice, while the other Zr ions segregate to form monoclinic/tetragonal ZrO_2 phases.¹⁵ The amount of the dissolved Zr ions in TiN, which is known to precisely control Φ ,³² was not well controlled by using the synthesis route used in this study. Further optimisation of the Zr-precursor and synthesis pathway is thus needed to further improve the ORR selectivity.

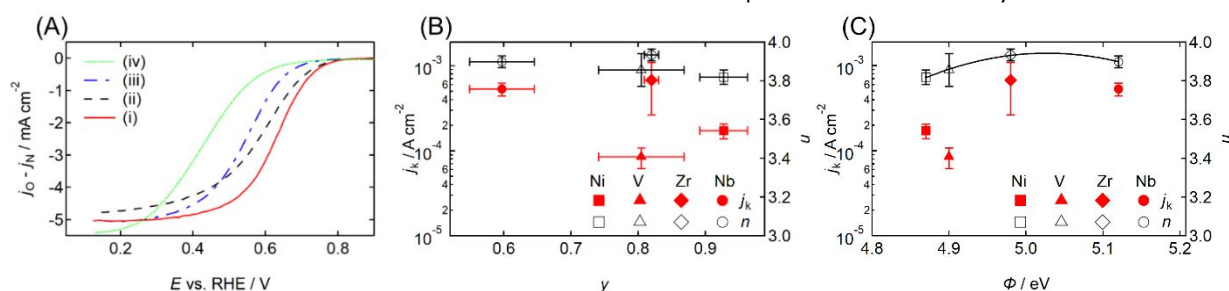


Fig. 3 (A) Rotating disk electrode (RDE) voltammograms of four $\text{Ti}_{0.8}\text{M}_{0.2}\text{O}_x\text{N}_y$ catalysts, where M = (i) Zr,¹⁴ (ii) Nb, (iii) Ni and (iv) V. The scans were performed under N_2 and O_2 atmospheres at a rotation speed of 1500 rpm and a cathodic scan rate of -5 mV s^{-1} in $0.1 \text{ mol dm}^{-3} \text{ H}_2\text{SO}_4$. The catalyst loading was constant at 0.86 mg cm^{-2} . (B) Kinetic current density and number of electrons transferred per unit oxygen molecules *versus* the nitrogen doping level in oxide surface curves (j_k - y and n - y curves, respectively). (C) j_k and n *versus* the work function, Φ , curves.

PCCP

COMMUNICATION

Conclusions

The effect of foreign-metal doping on the ORR reactivity of TiN catalysts was investigated. Independent of the doped metals, amorphous oxide layers were formed on the TiN surface and the selectivity was controlled by the work function. Among the four metals investigated herein, Zr was the best at improving the ORR selectivity by efficiently donating electrons to O₂ molecules, as its work function can be tuned to around 5.0 eV. Furthermore, the morphology of the Zr-doped TiN particles was fine and uniform, enhancing the ORR activity.

Author Contributions

M. C. worked on conceptualisation, synthesis, physical and chemical characterisation, data curation, formal analysis, funding acquisition, investigation and writing (original draft). T. A. and H. D. worked on investigation and writing (review and editing). X. R. and S. M. worked on writing (review and editing).

Conflicts of interest

There are no conflicts to declare.

Acknowledgements

The authors acknowledge Mr Yusei Tsushima, Ms Tomoko Numata and Dr Yoshiyuki Nakajima for obtaining the FE-SEM images/EDS mappings, UV-Raman spectra and work functions, respectively. This work was partially supported by JSPS KAKENHI Grant Numbers JP20K04299 and JP20H00220, and by the Takahashi industrial and economic research foundation, Japan and by JST, CREST Grant Number JPMJCR20B5, Japan. Some of the work was conducted at the Advanced Characterization Nanotechnology Platform of the University of Tokyo and supported by the “Nanotechnology Platform” of the MEXT, Japan, grant number JPMXP09A21UT0016.

Notes and references

- 1 D. A. Cullen, K. C. Neyerlin, R. K. Ahluwalia, R. Mukundan, K. L. More, R. L. Borup, A. Z. Weber, D. J. Myers and A. Kusoglu, *Nat. Energy*, 2021, **6**, 462.
- 2 M. M. Whiston, I. L. Azevedo, S. Litster, K. S. Whitefoot, C. Samaras and J. F. Whitacre, *Proc. Natl. Acad. Sci. USA*, 2019, **116**, 4899.
- 3 U. S. DRIVE Fuel Cell Technical Team Roadmap. https://www.energy.gov/sites/prod/files/2017/11/f46/FCTT_Roadmap_Nov_2017_FINAL.pdf (last accessed on June 16, 2022).
- 4 A. Kongkanand and M. Mathias, *J. Phys. Chem. Lett.*, 2016, **7**, 1127.
- 5 M. Lefèvre, E. Proietti, F. Jaouen and J. P. Dodelet, *Science*, 2009, **324**, 71; E. Proietti, F. Jaouen, M. Lefèvre, N. Larouche, J. Tian, J. Herranz and J. P. Dodelet, *Nat. Commun.*, 2011, **2**, 416.
- 6 J. Shui, C. Chen, L. Grabstanowicz, D. Zhao and D. J. Liu, *Proc. Natl. Acad. Sci. U. S. A.*, 2015, **112**, 10629; J. Li, M. Chen, D. A. Cullen, S. Hwang, M. Wang, B. Li, K. Liu, S. Karakalos, M. Lucero, H. Zhang, C. Lei, H. Xu, G. E. Sterbinsky, Z. Feng, D. Su, K. L. More, G. Wang, Z. Wang and G. Wu, *Nat. Catal.*, 2018, **1**, 935; X. Xie, C. He, B. Li, Y. He, D. A. Cullen, E. C. Wegener, A. J. Kropf, U. Martinez, Y. Cheng, M. H. Engelhard, M. E. Bowden, M. Song, T. Lemmon, X. S. Li, Z. Nie, J. Liu, D. J. Myers, P. Zelenay, G. Wang, G. Wu, V. Ramani and Y. Shao, *Nat. Catal.*, 2020, **3**, 1044; L. Jiao, J. Li, L. L. Richard, Q. Sun, T. Stracensky, E. Liu, M. T. Sougrati, Z. Zhao, F. Yang, S. Zhong, H. Xu, S. Mukerjee, Y. Huang, D. A. Cullen, J. H. Park, M. Ferrando, D. J. Myers, F. Jaouen and Q. Jia, *Nat. Mater.*, 2021, **20**, 1385.
- 7 R. Chenitz, U. I. Kramm, M. Lefèvre, V. Glibin, G. Zhang, S. Sun and J. P. Dodelet, *Energy Environ. Sci.*, 2018, **11**, 365.
- 8 Z. Xue, X. Zhang, J. Qin and R. Liu, *J. Energy Chem.*, 2021, **55**, 437.
- 9 M. Chisaka, in *Electrocatalysts for Low Temperature Fuel Cells: Fundamentals and Recent Trends*, ed. T. Maiyalagan and V. S. Saji, Wiley-VCH, Weinheim, 2017, p. 423.
- 10 Y. Liu, A. Ishihara, S. Mitsushima, N. Kamiya and K. Ota, *Electrochim. Solid-State Lett.*, 2005, **8**, A400; J. H. Kim, A. Ishihara, S. Mitsushima, N. Kamiya and K. Ota, *Electrochim. Acta*, 2007, **52**, 2492; A. Ishihara, S. Doi, S. Mitsushima and K. Ota, *Electrochim. Acta*, 2008, **53**, 5442; M. Chisaka, T. Iijima, T. Yaguchi and Y. Sakurai, *Electrochim. Acta*, 2011, **56**, 4581.
- 11 G. Liu, H. M. Zhang, M. R. Wang, H. X. Zhong and J. Chen, *J. Power Sources*, 2007, **172**, 503; M. Chisaka, Y. Suzuki, T. Iijima, Y. Ishihara, R. Inada and Y. Sakurai, *ECS Electrochem. Lett.*, 2012, **1**, F4; M. Chisaka, H. Sasaki and H. Muramoto, *Phys. Chem. Chem. Phys.*, 2014, **16**, 20415; M. Chisaka, A. Ishihara, N. Uehara, M. Matsumoto, H. Imai and K. Ota, *J. Mater. Chem. A*, 2015, **3**, 16414; G. Zhang, D. Sebastián, X. Zhang, Q. Wei, C. Lo Vecchio, J. Zhang, V. Baglio, W. Wang, S. Sun, A. S. Aricò and A. C. Tavares *Adv. Energy Mater.*, 2020, **10**, 2000075.
- 12 M. Chisaka, A. Ishihara, H. Morioka, T. Nagai, S. Yin, Y. Ohgi, K. Matsuzawa, S. Mitsushima and K. Ota, *ACS Omega*, 2017, **2**, 678.
- 13 M. Chisaka, Y. Ando and H. Muramoto, *Electrochim. Acta*, 2015, **183**, 100; M. Chisaka, Y. Ando and N. Itagaki, *J. Mater. Chem. A*, 2016, **4**, 2501.
- 14 M. Chisaka, Y. Ando, Y. Yamamoto and N. Itagaki, *Electrochim. Acta*, 2016, **214**, 165; M. Chisaka, Y. Yamamoto, N. Itagaki and Y. Hattori, *ACS Appl. Energy Mater.*, 2018, **1**, 211; M. Chisaka and H. Morioka, *Catal. Sci. Technol.*, 2019, **9**, 611; M. Chisaka, R. Xiang, S. Maruyama and H. Daiguji, *ACS Appl. Energy Mater.*, 2020, **3**, 9866.
- 15 M. Chisaka, R. Xiang, S. Maruyama and H. Daiguji, *Energy Fuels*, 2022, **36**, 539.

- 16 Y. Yang, L. Lai, L. Wei and Y. Chen, *J. Energy Chem.*, 2021, **63**, 667.
- 17 S. Chang and R. Doong, *J. Phys. Chem. B*, 2006, **110**, 20808; J. Lukáč, M. Klementová, P. Bezdička, J. Šubrt, L. Szatmáry, Z. Bastlb, J. Jirkovský, *Appl. Catal. B*, 2007, **74**, 83; L. Li, C. Li and Y. Liu, *Mater. Chem. Phys.*, 2009, **113**, 551; G. Abadias, L.E. Koutsokeras, A. Siozios and P. Patsalas, *Thin Solid Films*, 2013, **538**, 56; V. Molinari, C. Giordano, M. Antonietti, and D. Esposito, *J. Am. Chem. Soc.*, 2014, **136**, 1758.
- 18 M. Chisaka, *Phys. Chem. Chem. Phys.*, 2018, **20**, 15613.
- 19 R. D. Shannon, *Acta Crystallogr., Sect. A*, 1976, **32**, 751; S. Jeon, J. Ryu, H. G. Shin, J. Lee and H. Lee, *Mater. Charact.*, 2017, **131**, 374.
- 20 M. Li, Z. Feng, G. Xiong, P. Ying, Q. Xin and C. Li, *J. Phys. Chem. B*, 2001, **105**, 8107; J. Zhang, M. Li, Z. Feng, J. Chen, and C. Li, *J. Phys. Chem. B*, 2006, **110**, 927.
- 21 E. Nardou, D. Vouagner, A. M. Jurdyc, A. Berthelot, A. Pillonnet, V. Sablonière, F. Bessueille and B. Champagnon, *J. Non-Cryst. Solids*, 2011, **357**, 1895.
- 22 T. Yao and H. Wang, *J. Colloid Interface Sci.*, 2021, **604**, 188.
- 23 J. H. Chang, Y. L. Wang, C. D. Dong and S. Y. Shen, *Catalysts*, 2020, **10**, 482.
- 24 A. Ohma, K. Shinohara, A. Iiyama, T. Yoshida and A. Daimaru, *ECS Trans.*, 2011, **41**, 775.
- 25 J. Y. Cheon, J. H. Kim, J. H. Kim, K. C. Goddeti, J. Y. Park and S. H. Joo, *J. Am. Chem. Soc.*, 2014, **136**, 8875.
- 26 M. Sharma, J. H. Jang, D. Y. Shin, J. A. Kwon, D. H. Lim, D. Choi, H. Sung, J. Jang, S. Y. Lee, K. Y. Lee, H. Y. Park, N. Jung and S. J. Yoo, *Energy Environ. Sci.*, 2019, **12**, 2200.
- 27 R. Nandan, P. Pandey, A. Gautam, O. Y. Bisen, K. Chattopadhyay, M. M. Titirici and K. K. Nanda, *ACS Appl. Mater. Interfaces*, 2021, **13**, 3771.
- 28 H. Shin, N. Kang, D. Kang, J. S. Kang, J. H. Ko, D. H. Lee, S. Park, S. Uk Son and Y. E. Sung, *ChemElectroChem*, 2018, **5**, 1905.
- 29 X. Zhao, L. Wang, X. Chen, W. Wang, H. L. Xin, X. Du and J. Yang, *J. Power Sources*, 2020, **449**, 227482.
- 30 M. García-Mota, A. Vojvodic, H. Metiu, I. C. Man, H. Y. Su, J. Rossmeisl and J. K. Nørskov, *ChemCatChem*, 2011, **3**, 1607.
- 31 S. Trasatti, *Pure & App. Chem.*, 1986, **58**, 955.
- 32 G. M. Matenoglou, L. E. Koutsokeras and P. Patsalas, *Appl. Phys. Lett.*, 2009, **94**, 152108.